ISSN 1063-7834, Physics of the Solid State, 2019, Vol. 61, No. 3, pp. 361–369. © Pleiades Publishing, Ltd., 2019.
Russian Text © V.A. Orlov, A.A. Ivanov, I.N. Orlova, 2019, published in Fizika Tverdogo Tela, 2019, Vol. 61, No. 3, pp. 493–500.

MAGNETISM

Motion of Coupled Magnetic Vortices in Parallel Nanostripes

V. A. Orlov[a, b, *], A. A. Ivanov[a], and I. N. Orlova[c]

[a] *Siberian Federal University, Krasnoyarsk, 660041 Russia*
[b] *Kirensky Institute of Physics, Krasnoyarsk Scientific Center, Siberian Branch, Russian Academy of Sciences, Krasnoyarsk, 660036 Russia*
[c] *Krasnoyarsk State Pedagogical University, Krasnoyarsk, 660060 Russia*
**e-mail: e.orlhome@rambler.ru*

Received October 18, 2018

Abstract—The periodic motion of the interacting vortex domain walls in a pair of nanostripes has been theoretically investigated. As a model, two parallel nanostripes with magnetization inhomogeneities in the form of magnetic vortices have been examined. The magnetic subsystems of the stripes are magnetostatically coupled. The quasi-elastic coupling between vortices ensures the existence of normal modes of the periodic magnetization motion. The frequencies of these modes have been calculated. It is shown that not any combination of the vortex topological charge leads to the resonant behavior of magnetization in ac fields. The effect of the static component of a magnetic field on the frequency of the periodic motion of vortex domain walls is discussed.

DOI: 10.1134/S1063783419030223

1. INTRODUCTION

The attention to low-dimensional objects, including nanowires and nanostripes, is caused not only by the prospects for designing various spintronic devices [1–3], but also by the possibility of solving many fundamental problems of magnetism. The magnetization switching processes have been in focus. At the same time, an analytical description of the magnetic properties of nanostripes faces great computational difficulties related to the complex magnetization structure and specific features of the behavior in ac fields. Therefore, the evolution of the domain structure of nanostripes under the action of an ac magnetic field evokes particular interest.

Depending on the stripe geometry, i.e., the ratio between linear sizes, and the magnetic characteristics, various types of domain walls (DWs) have been implemented, including the conventional Neel-type transverse walls (TWs), vortex wall (VWs), and their complex combinations [4–11]. Different types of DWs in stripes have been intensively studied both theoretically (for example, [10, 12]) and experimentally (for example, [13, 14]). Certainly, the motion of walls with such complex configurations is characterized by extraordinary effects and evokes the interest of researchers. In particular, several modes of motion of the walls with a vortex structure under the action of a static field (or spin-polarized current), depending on its value, have been discovered and studied fairly well [15–20]. Interestingly, the presence of a vortex structure causes the cyclic motion of a wall with a shift (drift).

In arrays of closely adjacent wires (stripes), the mutual effect of their magnetic subsystems cannot be excluded. There is a significant coupling between topological inhomogeneities of magnetization, which affects the magnetization switching [21, 22]. The aim of this study was to describe the cyclic motion of vortex walls in a pair of magnetostatically coupled nanostripes under the action of an ac magnetic field applied in the stripe plane. In addition, we discuss the effect of a dc magnetic field applied perpendicular to the stripe plane.

The formalism in describing the behavior of magnetic vortices as topological inhomogeneities in ac fields is fairly well developed (see, for example, [23–30] and references therein). The analytical calculations are based on the representation of the Landau–Lifshitz equation through collective variables [30–32]. The role of such variables is played by the velocity and coordinates of the magnetic vortex center (core). The core is a region with a strongly inhomogeneous magnetization perpendicular to the magnet surface. In a magnetic field, the core behaves like a quasiparticle. The core forms as a result of the competition between the exchange and magnetostatic energy.

The vortex magnetization state is conventionally specified by two parameters: the core polarity $p = \pm 1$ and the core chirality $q = \pm 1$. The polarity sign is specified conditionally: along or opposite to the stripe surface normal. The chirality sign is also conventional; the magnetization rotates clockwise or counterclockwise. It is often convenient to use the topological

charge $\pi_T = pq$ to specify the vortex magnetic state. The character of the core motion in nanomagnets is such as if the core quasiparticle is affected by the gyroscopic force $\mathbf{F}_G = \mathbf{G} \times \mathbf{v}$ [30]. Here, $\mathbf{G}$ is the gyrovector and $\mathbf{v}$ is the core velocity. The gyrovector is expressed as $|\mathbf{G}| = \pi_T(2\pi M_S b/\gamma)(1 - ph)$, where b is the magnet thickness, γ is the gyromagnetic ratio, M_S is the saturation magnetization, and $h = H/(\mu_0 M_S)$ is the dimensionless field applied perpendicular to the magnetic plane (along or against the magnetization at the core center) [26, 32]. The vortex wall in wires and stripes is also affected by this force.

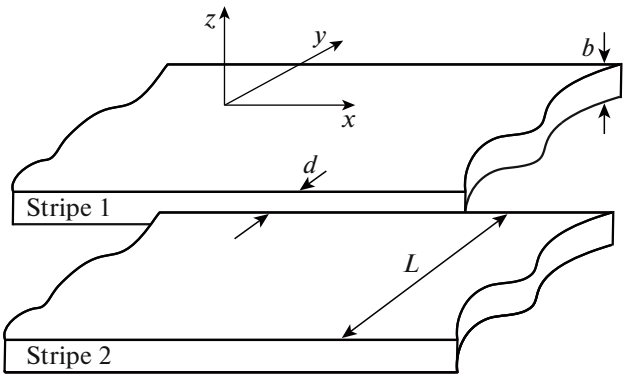

Fig. 1. Model of a pair of parallel nanostripes.

2. EFFECTIVE ENERGY OF A VORTEX DOMAIN WALL IN THE STRIPE

To solve the equation of motion of the magnetization, it is necessary to obtain a functional dependence of the potential energy of the stripe magnetic subsystem on generalized parameters. A rigorous analytical dependence of the energy on the vortex core coordinates is difficult to obtain. In such systems, the energy of interacting vortex walls can be, at best, approximated by a system of interacting dipoles or quadrupoles. In this approximation, the energy is expressed through complex integrals (see, for example, [12]), but, near the equilibrium, the energy is quadratic in the wall coordinates [16]. Often, practically important results are obtained by computer simulation [6, 16, 17, 33–35].

Let us write an empirical expression for the potential energy as a function of the core coordinate $W_M(\mathbf{r})$. We investigate a model consisting of two parallel ferromagnetic stripes with thickness b and width L ($b \ll L$). The spacing between stripes is d. The stripe length is much greater than the width and thickness. The coordinate system and model used are shown in Fig. 1. The magnetization distribution in nanostripes in the presence of a domain structure results from the competition of several types of energy, including exchange, demagnetization, anisotropy, etc. In general, a domain wall can include areas with the conventional Neel magnetization switching and a vortex part [36, 37].

An example of the characteristic magnetization distribution is shown in Fig. 2. In the figure, the arrow lengths are proportional to the projection of the magnetization unit vector onto the xy plane. The parameter $s = \pm 1$ conditionally denotes the magnetization configuration of neighboring domains, i.e., the direction toward the vortex or opposite. Note that the concept of a configuration of the magnetic field of a magnetostatic charge on the lateral stripe surface as of a quadrupole (composite charge/dipole/quadrupole systems) is not quite correct. The charge localization region on the side surfaces is fairly large (as compared with the stripe width L). It can be seen that the surface charge density σ on the side surface is noticeably different in absolute value in the regions with positive and negative signs. The areas with the higher density are marked in Fig. 2 with double signs "++" and "––" and the areas with the lower density, with single signs "+" and "–". The observations of the field distribution in real stripes also revealed this property [13].

The conservative forces acting on the core occur according to the following mechanism. At the shift of the vortex core, the surface charge density distribution on the side surfaces of the stripes changes. This leads to the change in the intrinsic energy of the stripes and their magnetostatic interaction W_M. Consequently, the effective forces acting on the vortex cores in stripes 1 and 2, as quasiparticles, can be written in the form $\mathbf{F}_\alpha(\mathbf{r}_1, \mathbf{r}_2) = -\text{grad}_\alpha(W_M(\mathbf{r}_1, \mathbf{r}_2))$ (subscript α is the stripe number and $\mathbf{r}_1$ and $\mathbf{r}_2$ are the radius vectors of the vortex centers). In estimations, the hard vortex model was approved. It consists in ignoring the change in the magnetization distribution profile at the minor change in the core coordinate [38–44]. In the framework of this model, for the energy of a magnetic subsystem of a pair of stripes, we obtain

$$W_M(x_1, y_1, x_2, y_2) = W_{1_{\text{self}}}(x_1, y_1) + W_{2_{\text{self}}}(x_2, y_2) + W_{\text{int}}(x_1, y_1, x_2, y_2). \quad (1)$$

In the right-hand side of Eq. (1), the first term $W_{1_{\text{self}}}(x_1, y_1)$ describes the intrinsic energy of stripe 1. The quantity $W_{2_{\text{self}}}(x_2, y_2)$ is the intrinsic energy of stripe 2 and $W_{\text{int}}(x_1, y_1, x_2, y_2)$ is the term describing the interaction between magnetic subsystems of the stripes. At small shifts from the equilibrium position, the total energy can be presented in the form

$$W_M(x_1, y_1, x_2, y_2) = \frac{1}{2}\chi(y_1 - y_{0_1})^2 + \frac{1}{2}\chi(y_2 - y_{0_2})^2 + w_0 f_x(\Delta x) f_y(\Delta y). \quad (2)$$

Here, χ is the rigidity of the magnetic subsystem of isolated stripes; $\Delta x = x_2 - x_1 - (x_{0_2} - x_{0_1})$; $\Delta y = y_2 - y_1 - (y_{0_2} - y_{0_1})$; y_1, y_2, x_1, and x_2 are the vortex core coordinates; y_{0_1}, y_{0_2}, x_{0_1}, and x_{0_2} are the vortex core

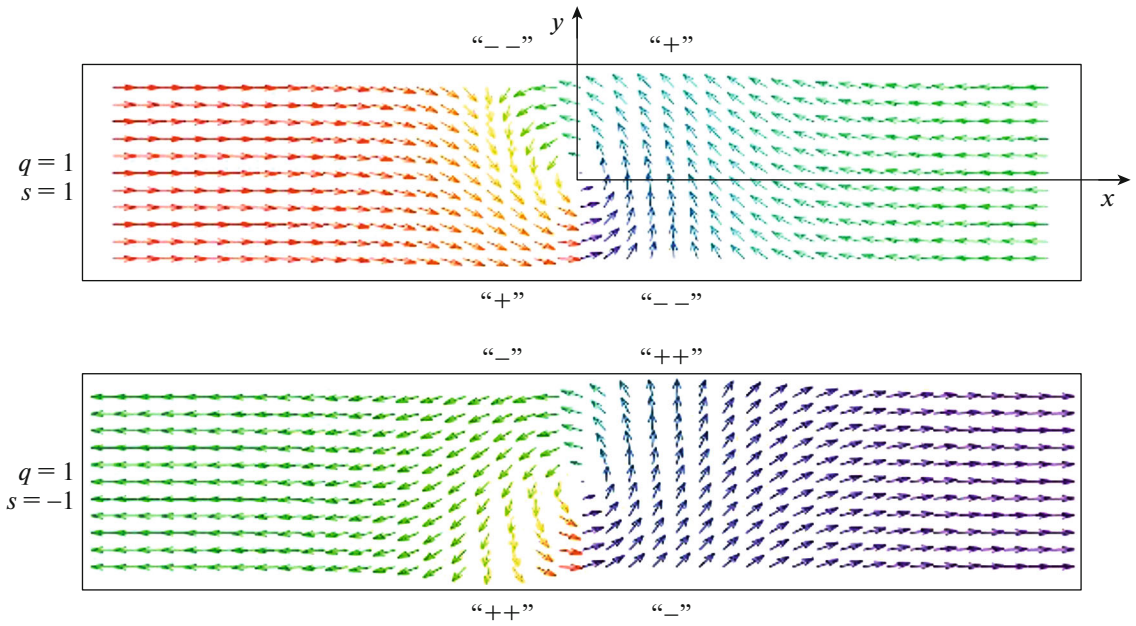

Fig. 2. Example of the magnetization distribution in a vortex wall at different combinations of parameters q and s. The distributions are built for the case of $\delta_w = L$ and $\delta_c = 0.2\delta_w$.

coordinates in the equilibrium positions; and w_0 is the constant determined by the magnetic characteristics of a system. The functions $f(\Delta x)$ and $f(\Delta y)$ should monotonically decrease with an increase in the absolute values $|\Delta x|$ and $|\Delta y|$, respectively.

This expression for the system energy was chosen for the following reasons. The energy of the magnetostatic interaction between charges on the side surfaces of an isolated stripe only depends on the coordinate y, since the charge distribution (and, hence, the energy) only changes when the core is shifted in the transverse direction. The third term is responsible for the energy of interaction between charges on the surfaces of different stripes. This energy depends on the difference between the vortex center coordinates, along both the y and x axis. It is important that the effective stiffness of the core coupling along the y axis depends on the distance between them along the x axis, and vice versa. Therefore, the functions f must decrease and depend on the arguments Δx and Δy in even powers. At small shifts, the functions f can be expanded in a series in powers of the arguments and, accurate to the second order, presented in the form

$$f_x(\Delta x) \approx \left(1 - \frac{\kappa_x \Delta x^2}{2w_0}\right), \quad f_y(\Delta y) \approx \left(1 - \frac{\kappa_y \Delta y^2}{2w_0}\right). \quad (3)$$

Here, κ_x and κ_y are the core coupling stiffnesses at the shift along the x and y axis, respectively.

A particular case of Eq. (2) for uncoupled stripes is in satisfactory agreement with the results reported in [6, 15, 16, 45]. In further calculations, we use this expression under the assumption of small core shifts,.

3. CYCLIC MOTION OF A VORTEX WALL

Let us now consider the behavior of a vortex core in an ac magnetic field applied in the stripe plane. To describe the dynamic behavior of magnetic vortices, it is efficient to use the Thiele equation [31]. The system of Thiele equations as applied to the vortex walls has the form

$$\begin{cases} \mathbf{G}_1 \times \mathbf{v}_1 - D\mathbf{v}_1 - \nabla W_1 = 0, \\ \mathbf{G}_2 \times \mathbf{v}_2 - D\mathbf{v}_2 - \nabla W_2 = 0. \end{cases} \quad (4)$$

Here, $\mathbf{G}_\alpha = \pi_{T_\alpha} G_0 (1 - p_\alpha h)\mathbf{k}$ is the gyrovector ($\mathbf{k}$ is the unit vector along the z axis, and $G_0 = 2\pi M_S b/\gamma$), $\mathbf{v}$ is the core velocity, M_S is the saturation magnetization, γ is the gyromagnetic ratio, b is the ribbon thickness, and D is the effective viscous friction coefficient. The subscripts indicate the stripe a vortex belongs to. The third term in the left-hand side of Eq. (4) is responsible for the conservative forces acting on the vortex core as a quasiparticle. Such forces include the restoring force, force of interaction with the vortex core of the neighboring stripe, and effective force acting on the core due to the interaction between the vortex magnetization and an external magnetic field. Thus, $W_\alpha = W_M(\mathbf{r}_1, \mathbf{r}_2) + W_{\alpha_H}$. Here, W_{α_H} is the Zeeman energy of a vortex domain wall in the stripe with number α.

Then, with regard to (2), for generalized forces acting on the vortex cores, we may write (**i** and **j** are the unit vectors along the x and y axis, respectively)

$$\mathbf{F}_\alpha(\mathbf{r}_1, \mathbf{r}_2) = -\nabla W_\alpha = -\kappa_x \Delta x \mathbf{i} - \kappa_y \Delta y \mathbf{j} - \chi y_\alpha \mathbf{j} + \mathbf{F}_{\alpha_H}. \quad (5)$$

The force $\mathbf{F}_{\alpha_H}$ acting on the core, due to the presence of an ac magnetic field, is perpendicular to the direction of this field and lies in the stripe plane. A specific direction of this force is determined by the vortex chirality q_α [46, 47]. Note that the dc magnetic field applied perpendicular to the stripe plane determines the parameters $\mathbf{G}_\alpha$, κ_x, κ_y, and χ.

In the projection onto the system of coordinates (local for each stripe), system (4) takes the form

$$\begin{cases} -G_1 v_{y_1} - D v_{x_1} - \kappa_x (x_1 - x_2) = -F_{1_x}, \\ G_1 v_{x_1} - D v_{y_1} - \kappa_y (y_1 - y_2) - \chi y_1 = -F_{1_y}, \\ -G_2 v_{y_2} - D v_{x_2} - \kappa_x (x_2 - x_1) = -F_{2_x}, \\ G_2 v_{x_2} - D v_{y_2} - \kappa_y (y_2 - y_1) - \chi y_2 = -F_{2_y}. \end{cases} \quad (6)$$

Here, F_{α_x} and F_{α_y} are the x and y projections of the forces $\mathbf{F}_{\alpha_H}$ acting on the vortex cores. Let the ac field be changing in accordance with the law $\mathbf{F}_{\alpha_H} = q_\alpha \mathbf{F}_0 (\exp(i\omega t) + \exp(-i\omega t))$, where ω is the cyclic frequency of the field variation and $\mathbf{F}_0$ is the field amplitude.

We choose the trial solutions of system (6) in the form

$$\begin{cases} x_\alpha = x_{0_\alpha} (\exp(i\pi_{T_\alpha} \omega t + \phi_{\alpha_x}) + \exp(-i\pi_{T_\alpha} \omega t - \phi_{\alpha_x})), \\ y_\alpha = i y_{0_\alpha} (\exp(i\pi_{T_\alpha} \omega t + \phi_{\alpha_y}) - \exp(-i\pi_{T_\alpha} \omega t - \phi_{\alpha_y})). \end{cases} \quad (7)$$

Here, i is the imaginary unit and $\phi_{\alpha_{x,y}}$ is the phase difference between the law of variation in the force $\mathbf{F}_{\alpha_H}$ and the law of variation in the coordinates x and y, respectively. Then, substituting the trial solutions to Eq. (6), in the steady-state regime we obtain

$$\begin{cases} G_0(1 - p_1 h)\omega y_{0_1} - (\kappa_x + iD\omega) x_{0_1} - \kappa_x x_{0_2} = F_{0_x} q_1, \\ G_0(1 - p_1 h)\omega x_{0_1} - (\kappa_y + \chi + iD\omega) y_{0_1} \\ - \pi_{T_1}\pi_{T_2} \kappa_y y_{0_2} = -i\pi_{T_1} F_{0_y} q_1, \\ G_0(1 - p_2 h)\omega y_{0_2} - (\kappa_x + iD\omega) x_{0_2} - \kappa_x x_{0_1} = F_{0_x} q_2, \\ G_0(1 - p_2 h)\omega x_{0_2} - (\kappa_y + \chi + iD\omega) y_{0_2} \\ - \pi_{T_1}\pi_{T_2} \kappa_y y_{0_1} = -i\pi_{T_2} F_{0_y} q_2. \end{cases} \quad (8)$$

The solution of this system allows us to determine the complex amplitudes

$$x_{0_1} = -\frac{C_x}{G_0(1 - p_1 h)^3 (1 - p_2 h)^3 Z}, \qquad y_{0_1} = -\frac{C_y}{G_0(1 - p_1 h)^3 (1 - p_2 h)^3 Z}. \quad (9)$$

Here, we made the designations

$$\begin{aligned} C_x &= [F_{0_x}(q_1(\omega_y + \Omega + i\omega\omega_\Gamma)(1 - p_2 h) \\ &- p_2 \pi_{T_1} \omega_y (1 - p_1 h)) - iF_{0_y} p_1 \omega (1 - p_1 h)(1 - p_2 h)] \\ &\times [(\omega_x + i\omega\omega_\Gamma)(\omega_y + \Omega + i\omega\omega_\Gamma)(1 - p_1 h) \\ &+ \pi_{T_1}\pi_{T_2} \omega_x \omega_y (1 - p_2 h) - \omega^2 (1 - p_1 h)(1 - p_2 h)^2] \\ &+ [F_{0_x}(q_2(\omega_y + \Omega + i\omega\omega_\Gamma)(1 - p_1 h) \\ &- p_1 \pi_{T_2} \omega_y (1 - p_2 h)) - iF_{0_y} p_2 \omega (1 - p_1 h)(1 - p_2 h)] \\ &\times [\omega_x(\omega_y + \Omega + i\omega\omega_\Gamma)(1 - p_2 h) \\ &+ \pi_{T_1}\pi_{T_2} (\omega_x + i\omega\omega_\Gamma)\omega_y (1 - p_1 h)] \end{aligned} \quad (10)$$

and

$$\begin{aligned} C_y &= [F_{0_x}(q_1(\omega_y + \Omega + i\omega\omega_\Gamma)(1 - p_2 h) \\ &- p_2 \pi_{T_1} \omega_y (1 - p_1 h)) - iF_{0_y} p_1 \omega (1 - p_1 h)(1 - p_2 h)] \\ &\times [\omega_x(\omega_y + \Omega + i\omega\omega_\Gamma)(1 - p_1 h) \\ &+ \pi_{T_1}\pi_{T_2} \omega_y (\omega_x + i\omega\omega_\Gamma)(1 - p_2 h)] \\ &+ [F_{0_x}(q_2(\omega_y + \Omega + i\omega\omega_\Gamma)(1 - p_1 h) \\ &- p_1 \pi_{T_2} \omega_y (1 - p_2 h)) - iF_{0_y} p_2 \omega (1 - p_1 h)(1 - p_2 h)] \\ &\times [(\omega_x + i\omega\omega_\Gamma)(\omega_y + \Omega + i\omega\omega_\Gamma)(1 - p_2 h) \\ &+ \pi_{T_1}\pi_{T_2} \omega_x \omega_y (1 - p_1 h) - \omega^2 (1 - p_1 h)^2 (1 - p_2 h)], \end{aligned} \quad (11)$$

$$\begin{aligned} Z &= \omega^4 - \omega^2 \left[(\omega_x + i\omega\omega_\Gamma)(\omega_y + \Omega + i\omega\omega_\Gamma) \right. \\ &\times \left. \left(\frac{1}{(1 - p_1 h)^2} + \frac{1}{(1 - p_2 h)^2} \right) + \frac{2\pi_{T_1}\pi_{T_2}\omega_x\omega_y}{(1 - p_1 h)(1 - p_2 h)} \right] \\ &+ \frac{[(\omega_x + i\omega\omega_\Gamma)^2 - \omega_x^2][(\omega_y + \Omega + i\omega\omega_\Gamma)^2 - \omega_y^2]}{(1 - p_1 h)^2 (1 - p_2 h)^2}, \end{aligned} \quad (12)$$

where $\omega_\Gamma = D/G_0$ is the dimensionless quantity, $\Omega = \chi/G_0$, $\omega_x = \kappa_x/G_0$, and $\omega_y = \kappa_y/G_0$.

The phase difference between the laws of variation in the driving force and vortex core motion is determined as

$$\begin{cases} \sin(\phi_{\alpha_x}) = \dfrac{\mathrm{Im}(x_{0_\alpha})}{|x_{0_\alpha}|}, \\ \cos(\phi_{\alpha_x}) = \dfrac{\mathrm{Re}(x_{0_\alpha})}{|x_{0_\alpha}|}. \end{cases} \quad \begin{cases} \sin(\phi_{\alpha_y}) = \pi_{T_\alpha} \dfrac{\mathrm{Im}(y_{0_\alpha})}{|y_{0_\alpha}|}, \\ \cos(\phi_{\alpha_y}) = \pi_{T_\alpha} \dfrac{\mathrm{Re}(y_{0_\alpha})}{|y_{0_\alpha}|}. \end{cases} \quad (13)$$

The factor π_{T_α} takes into account the core rotation direction.

Table 1. Set of eigenfrequencies ω_s of the system calculated using Eq. (14) at different combinations of the vortex wall chiralities and polarities

No.	Combination of p_α and $q_\alpha\{p_1, p_2, q_1, q_2\}$	Collective mode frequency ω_s
1	$\{1, 1, \pm1, \pm1\}$	$\frac{2\omega_x(\Omega + 2\omega_y)}{(1-h)^2}$
2	$\{1, 1, \pm1, \mp1\}$	$\frac{2\omega_x\Omega}{(1-h)^2}$
3	$\{\pm1, \mp1, 1, 1\}, \{\pm1, \mp1, -1, -1\}$	$\frac{2\omega_x}{(1-h^2)^2}(\Omega(1+h^2) + 2\omega_y h^2)$
4	$\{\pm1, \mp1, 1, -1\}, \{\pm1, \mp1, -1, 1\}$	$\frac{2\omega_x}{(1-h^2)^2}(\Omega(1+h^2) + 2\omega_y)$
5	$\{-1, -1, \pm1, \pm1\}$	$\frac{2\omega_x(\Omega + 2\omega_y)}{(1+h)^2}$
6	$\{-1, -1, \pm1, \mp1\}$	$\frac{2\omega_x\Omega}{(1+h)^2}$

In the particular case of a negligible damping ($\omega_\Gamma = 0$), the eigenfrequencies of the modes can be easily determined from the condition $|Z| = 0$. As a result, we have

$$\omega_s^2 = \omega_x\Omega\left(\frac{1}{(1-p_1h)^2} + \frac{1}{(1-p_2h)^2}\right) + \omega_x\omega_y\left(\frac{\pi_{T_1}}{1-p_1h} + \frac{\pi_{T_2}}{1-p_2h}\right)^2. \quad (14)$$

The distribution of polarities, chiralities, and frequencies is given in Table 1. Since both stripes in a pair have the same size and magnetic characteristics, the G_0, D, and χ values of the stripes are the same. This leads to the frequency degeneracy of the states. In particular, each of the states with numbers 1, 2, 5, and 6 from Table 1 is doubly degenerate and states 3 and 4 are quadrupely degenerate. Thus, we have six eigenfrequencies.

In zero perpendicular dc field ($h = 0$), we obtain from Eq. (14) for the resonance frequencies:

$$\omega_s = \sqrt{2\omega_x\Omega + 2\omega_x\omega_y(1 + \pi_{T_1}\pi_{T_2})}. \quad (15)$$

The states with certain combinations of the chirality, but opposite polarities do not differ in the absence of field h. Consequently, at $\omega_\Gamma \to 0$, the degree of degeneracy increases. As a result, the sets of states {1, 4, 5} and, separately, {2, 3, 6} in Table 1 become indistinguishable. Note that in zero dc field h, it is not the difference between the polarities and chiralities that is important, but the difference between their product pq, i.e., topological charges π_{T_α}, which is reflected in formula (15) indicating that, at $h = 0$, there are only two different frequencies, $\omega_s = \sqrt{2\omega_x\Omega}$ and $\omega_s = \sqrt{2\omega_x\Omega + 4\omega_x\omega_y}$. Talbi et al. [48] theoretically investigated the dynamics of two interacting vortices within a single stripe and obtained a result for the frequency of collective motion of vortices, which is a particular case of formula (15).

The energy absorbed by a pair of stripes can be estimated by the formula

$$P(\omega, h) \approx D\omega^2(|x_{0_1}|^2 + |y_{0_1}|^2 + |x_{0_2}|^2 + |y_{0_2}|^2). \quad (16)$$

The dependence of the absorbed (dimensionless) power on the frequency of an external ac field applied along the y axis is shown in Fig. 3 and, along the x axis, in Fig. 4. These plots need our comments.

First of all, it is worth noting that, in the discussed stripe model, the long and vortex walls are distant from the ends. Therefore, the magnetic energy of an isolated stripe does not change when the vortex center shifts along the x axis. Hence, a returning force along the x axis does not occur. In an isolated stripe, during the shift of the vortex core along the y axis, the energy of the magnetic subsystem changes due to redistribution of magnetic charges on the side surfaces of the stripe. Consequently, the restoring force acting along the y axis occurs, regardless of the presence of the second stripe. This feature is reflected on the wall motion in an ac magnetic field.

The state illustrated in Fig. 3 does not exhibit the resonant properties. Depending on the mutual orientation of the perpendicular dc field h and core polarity p_α, we have the frequency dependences monotonically descending at different rates. The calculation of the phase difference between the wall core motion in stripes 1 and 2 using formulas (13) showed the synchronous rotation ($\phi_{1_x} = \phi_{2_x}$ and $\phi_{1_y} = \phi_{2_y}$). At such combinations of the vortex polarities and chiralities,

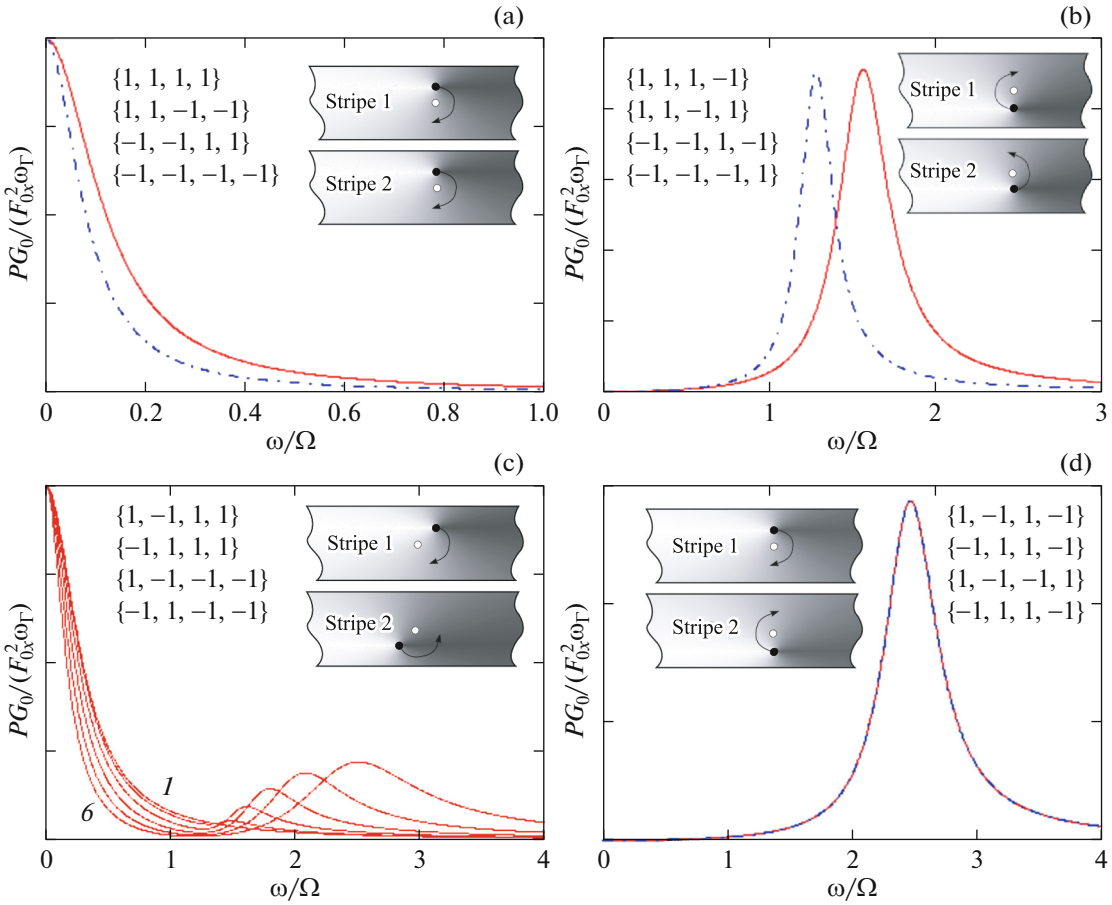

Fig. 3. Dependence of the absorbed power (dimensionless arb. units) on the ac field frequency. The ac field is applied along the *y* axis. The curves are plotted for the parameters $\omega_y = \Omega$, $\omega_x = \omega_y$, $\omega_\Gamma = 0.1$, and $h = 0.1$. (a, b) Dash-and-dot curves show the power for a dc field applied antiparallel to the *z* axis. (c, d) The cases of a dc field applied parallel and antiparallel the *z* axis coincide. (c) A set of curves *1*–*6* at dc fields of $h = 0$–0.5 with a step $\Delta h = 0.1$. Insets: combinations of polarities and chiralities of the vortex walls $\{p_1, p_2, q_1, q_2\}$ in braces and phases and directions of the vortex core motion. Black dots show the cores and white dots, the origin of coordinates.

the interaction between domain walls does not manifest itself, since the conditions $\Delta x = 0$ and $\Delta y = 0$ are met at any instant of time. In this case, the equations of motion contain no projection of the restoring force along the *x* axis and the system is not oscillatory.

A similar effect can be observed in the case of an ac field applied along the *y* axis (Figs. 4a, 4b). The calculation of phases for these combinations $\{p_1, p_2, q_1, q_2\}$ showed that the coordinates x_1 and x_2 change synchronously with time. This indicates the absence of a restoring force along the *x* axis.

The system behaves differently if the vortex center coordinates x_1 and x_2 change asynchronously with time. In this case, the generalized force of the interaction between the cores has a nonzero projection onto the *x* axis; i.e., there is a returning factor not only along the *y* axis, but also along the *x* axis. In this case, the system has the characteristics of a vibrational one and resonance states exist in an ac field. Such combinations $\{p_1, p_2, q_1, q_2\}$ are shown in Figs. 3b, 3c, 3d, 4c, and 4d. The inserts in the plots show the directions and phases of the vortex core motion at certain instants of time.

It is interesting to investigate the states with the same chiralities, but opposite polarities (Figs. 3c and 4c). When an ac field is applied along the *y* axis, the resonance peak only arises in the presence of a dc field perpendicular to the stripe plane. In an ac field applied along the *x* axis, the resonance is implemented at any values of the perpendicular field *h*. In these states, the phase shift between the vortex center positions in the stripes $\phi_{1_{x,y}} - \phi_{2_{x,y}}$ depends on the ac field frequency and dc field value. This dependence does not exist at the rest $\{p_1, p_2, q_1, q_2\}$ combinations, when there are only two possibilities: $\phi_{1_{x,y}} - \phi_{2_{x,y}} = 0, \pi$. The behavior of the core rotation phases in the stripes for the discussed case is illustrated in Fig. 5.

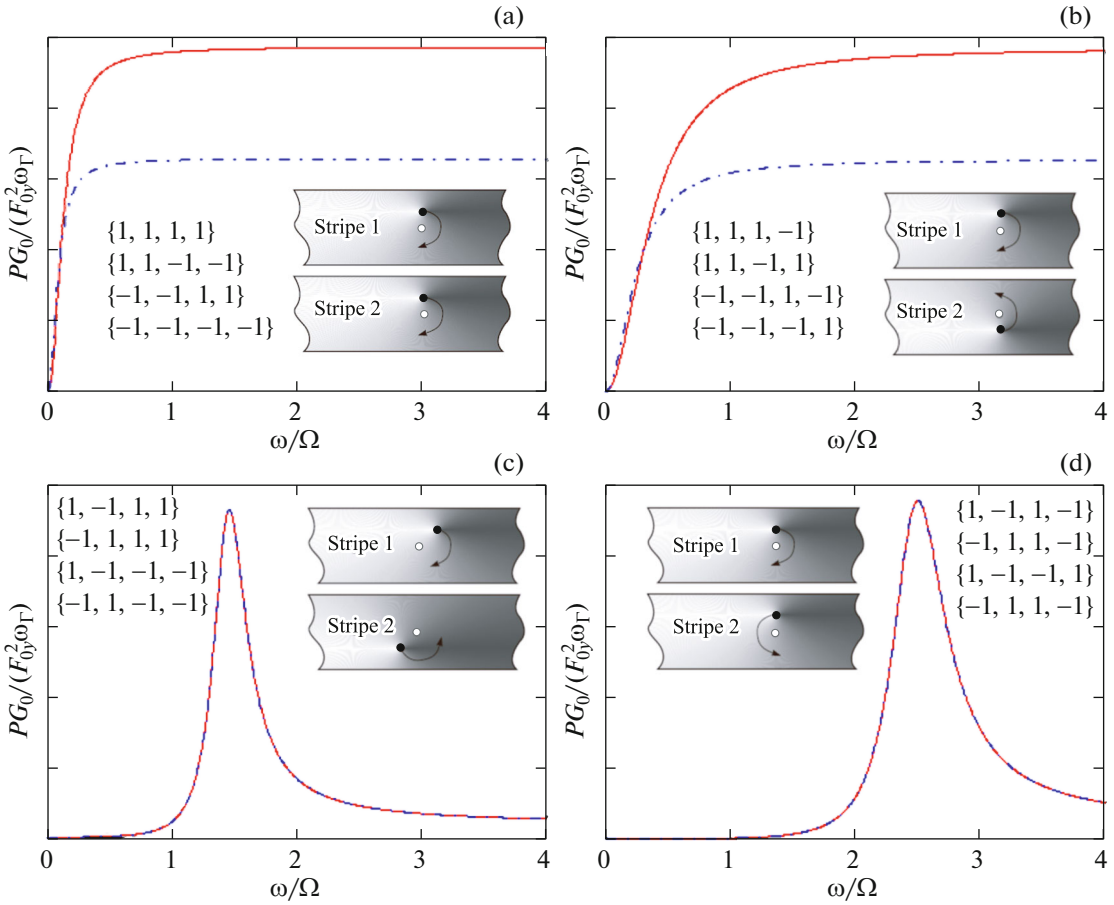

Fig. 4. Dependence of the absorbed power (arb. units) on the frequency of an ac field applied along the *x* axis. The curves are built for the same parameters as in Fig. 3.

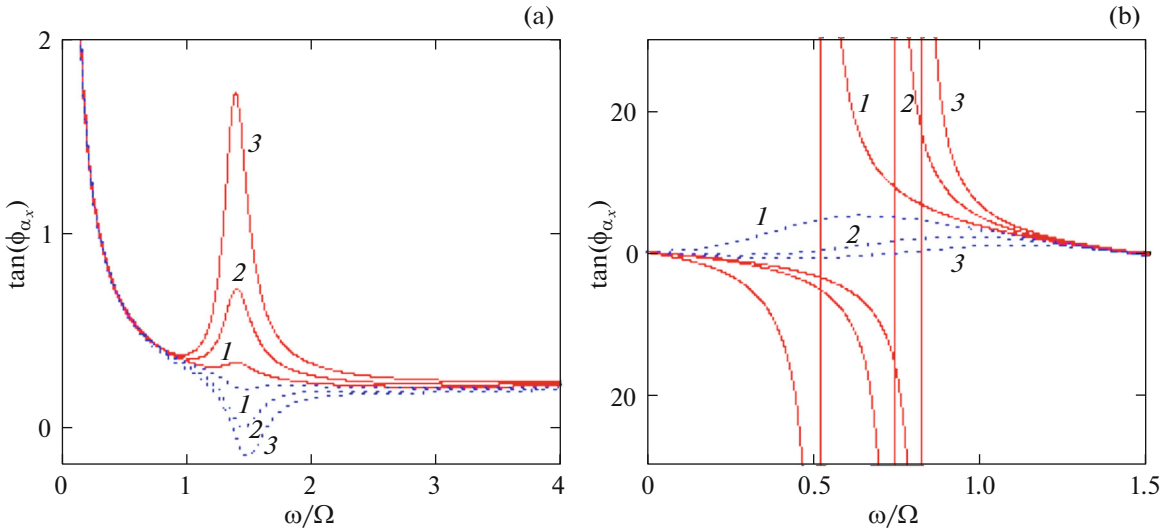

Fig. 5. Dependence of the coordinate-*x* phase tangent of the magnetic vortex core in stripe 1 (solid curves) and stripe 2 (dots). Curves *1*–*3* are plotted at different values of a perpendicular dc field: $h_1 = 0.01$, $h_2 = 0.05$, and $h_3 = 0.1$, respectively. The plot is built for an ac field applied along (a) the *y* and (b) *x* axis.

4. CONCLUSIONS

The analysis and solution of the equations of vortex motion showed that there are certain combinations of polarities and chiralities of vortex walls at which their motion is periodic. By ignoring the damping, a simple expression was obtained for the resonance frequencies as functions of the topological charge of the vortices and value and direction of a dc magnetic field perpendicular to the stripe surface.

The knowledge of the states of coupled vortex walls at which the resonance or nonresonance behavior in ac fields is implemented opens the opportunities for purposeful control of magnetization in arrays of parallel stripes. This is especially important for the development of data storage devices.

The field dependence of the frequencies of the modes of collective motion of vortex walls makes such systems good candidates for use in various field sensors and other spintronic devices. The existence of states with the resonance frequency sensitive to the perpendicular field direction (Fig. 3b) opens up the possibility of designing sensors that determine not only value, but also direction of the field.

ACKNOWLEDGMENTS

This study was supported by the Russian Foundation for Basic Research, project no. 18-02-00161.

REFERENCES

1. D. A. Allwood, G. Xiong, C. C. Faulkner, D. Atkinson, D. Petit, and R. P. Cowburn, Science (Washington, DC, U. S.) **309**, 1688 (2005).
2. M. Hayashi, L. Thomas, R. Moriya, Ch. Rettner, and S. S. P. Parkin, Science (Washington, DC, U. S.) **320**, 209 (2008).
3. S. S. P. Parkin, M. Hayashi, and L. Thomas, Science (Washington, DC, U. S.) **320**, 190 (2008).
4. S. Jamet, N. Rougemaille, J. C. Toussaint, and O. Fruchart, arXiv:1412.0679v1 [cond-mat.mes-hall] (2014).
5. A. Thiaville and Yo. Nakatani, Appl. Phys. **101**, 161 (2006).
6. H. Youk, G.-W. Chern, K. Merit, B. Oppenheimer, and O. Tchernyshyov, J. Appl. Phys. **99**, 08B101 (2006).
7. Yo. Nakatania, A. Thiavilleb, and J. Miltat, J. Magn. Magn. Mater. **290–291**, 750 (2005).
8. V. D. Nguyen, O. Fruchart, S. Pizzini, J. Vogel, J.-C. Toussaint, and N. Rougemaille, Sci. Rep. **5**, 12417 (2015).
9. N. Rougemaille, V. Uhlir, O. Fruchart, S. Pizzini, J. Vogel, and J. C. Toussaint, Appl. Phys. Lett. **100**, 172404 (2012).
10. A. K. Zvezdin, V. I. Belotelov, and K. A. Zvezdin, JETP Lett. **87**, 381 (2008).
11. V. V. Volkov and V. A. Bokov, Phys. Solid State **50**, 199 (2008).
12. A. Janutka, Acta Phys. Polon. A **124**, 641 (2013).
13. A. G. Kozlov, M. E. Stebliy, A. V. Ognev, A. S. Samardak, A. V. Davydenko, and L. A. Chebotkevich, J. Magn. Magn. Mater. **422**, 452 (2017).
14. M. Shen, Yue Zhang, L. You, and X. Yang, arxiv:1807.11063.
15. D. J. Clarke, O. A. Tretiakov, G.-W. Chern, Ya. B. Bazaliy, and O. Tchernyshyov, Phys. Rev. B **78**, 134412 (2008).
16. Y. Su, J. Sun, J. Hu, and H. Lei, Eur. Phys. Lett. **103**, 67004 (2013).
17. S.-K. Kim, J.-Y. Lee, Y.-S. Choi, K. Yu. Guslienko, and K.-S. Lee, Appl. Phys. Lett. **93**, 052503 (2008).
18. J. Yang, C. Nistor, G. S. D. Beach, and J. L. Erskine, Phys. Rev. B **77**, 014413 (2008).
19. K. Yu. Guslienko, J.-Y. Lee, and S.-K. Kim, IEEE Trans. Magn. **44**, 3079 (2008).
20. N. Locatelli, A. E. Ekomasov, A. V. Khvalkovskiy, Sh. A. Azamatov, K. A. Zvezdin, J. Grollier, E. G. Ekomasov, and V. Cros, Appl. Phys. Lett. **102**, 062401 (2013).
21. I. Purnama, M. Chandra Sekhar, S. Goolaup, and W. S. Lew, Appl. Phys. Lett. **99**, 152501 (2011).
22. Ch. Murapaka, S. Goolaup, I. Purnama, and W. S. Lewa, Appl. Phys. Lett. **117**, 053913 (2015).
23. O. Klein, G. de Loubens, V. V. Naletov, F. Boust, T. Guillet, H. Hurdequint, A. Leksikov, A. N. Slavin, V. S. Tiberkevich, and N. Vukadinovic, Phys. Rev. B **78**, 144410 (2008).
24. K.-S. Lee and S.-K. Kim, Appl. Phys. Lett. **91**, 132511 (2007).
25. B. A. Ivanov and G. M. Wysin, Phys. Rev. B **65**, 134434 (2002).
26. K. Yu. Guslienko, B. A. Ivanov, V. Novosad, Y. Otani, H. Shima, and K. Fukamichi, J. Appl. Phys. **91**, 8037 (2002).
27. V. A. Orlov, R. Yu. Rudenko, A. V. Kobyakov, A. V. Lukyanenko, P. D. Kim, V. S. Prokopenko, and I. N. Orlova, J. Exp. Theor. Phys. **126**, 523 (2018).
28. F. Abreu Araujo, M. Darques, K. A. Zvezdin, A. V. Khvalkovskiy, N. Locatelli, K. Bouzehouane, V. Cros, and L. Piraux, Phys. Rev. B **86**, 064424 (2012).
29. A. D. Belanovsky, N. Locatelli, P. N. Skirdkov, F. Abreu Araujo, J. Grollier, K. A. Zvezdin, V. Cros, and A. K. Zvezdin, Phys. Rev. B **85**, 100409(R) (2012).
30. A. K. Zvezdin and K. A. Zvezdin, Bull. Lebedev Phys. Inst. **37** (8), 240 (2010).
31. A. Thiele, Phys. Rev. Lett. **30**, 230 (1973).
32. J. Kim and S.-B. Choe, J. Magn. **12**, 113 (2007).
33. R. D. McMichael and M. J. Donahue, IEEE Trans. Magn. **33**, 4167 (1997).
34. O. A. Tretiakov, D. Clarke, Gia-Wei Chern, Ya. B. Bazaliy, and O. Tchernyshyov, Phys. Rev. Lett. **100**, 127204 (2008).
35. M. N. Dubovik, B. N. Filippov, and L. G. Korzunin, Phys. Met. Metallogr. **117**, 329 (2016).
36. G.-W. Chern, H. Youk, and O. Tchernyshyov, J. Appl. Phys. **99**, 08Q505 (2006).
37. J. He, Z. Li, and S. Zhang, Phys. Rev. B **73**, 184408 (2006).

38. U. K. Rossler, A. N. Bogdanov, and K.-H. Muller, IEEE Trans. Magn. **38**, 2586 (2002).
39. K. Yu. Guslienko, V. Novosad, Y. Otani, H. Shima, and K. Fukamichi, Phys. Rev. B **65**, 024414 (2001).
40. V. P. Kravchuk and D. D. Sheka, Phys. Solid State **49**, 1923 (2007).
41. P. D. Kim, V. A. Orlov, V. S. Prokopenko, S. S. Zamai, V. Ya. Prints, R. Yu. Rudenko, and T. V. Rudenko, Phys. Solid State **57**, 30 (2015).
42. K. Yu. Guslienko, X. F. Han, D. J. Keavney, R. Divan, and S. D. Bader, Phys. Rev. Lett. **96**, 067205 (2006).
43. M. Wolf, U. K. Robler, and R. Schafer, J. Magn. Magn. Mater. **314**, 105 (2007).
44. P. D. Kim, V. A. Orlov, R. Yu. Rudenko, V. S. Prokopenko, I. N. Orlova, and S. S. Zamai, JETP Lett. **101**, 562 (2015).
45. A. Janutka, Acta Phys. Polon. A **124**, 23 (2013).
46. S.-B. Choe, Y. Acremann, A. Scholl, A. Bauer, A. Doran, J. Stohr, and H. A. Padmore, Science (Washington, DC, U. S.) **304**, 420 (2010).
47. J. Y. Lee, K. S. Lee, S. Choi, K. Yu. Guslienko, and S.-K. Kim, Phys. Rev. B **76**, 184408 (2007).
48. Y. Talbi, Y. Roussigne, P. Djemia, and M. Labrune, J. Phys.: Conf. Ser. **200**, 042027 (2010).

Translated by E. Bondareva